A Mathematical Model for Trapping Skinning in Polymers

By David A. Edwards

When saturated polymer films are desorbed, a thin skin of glassy polymer can form at the exposed surface, inhibiting desorption. In addition, trapping skinning, in which an increase in the force driving the desorption decreases the accumulated flux, can also occur. These behaviors cannot be described by the simple Fickian diffusion equation. The mathematical model presented for the system is a moving boundary-value problem with a set of coupled partial differential equations that cannot be solved by similarity variables. Therefore, integral equation techniques are used to obtain asymptotic estimates for the solution. It is shown that although increasing the driving force will increase the instantaneous flux, the time of accumulation will decrease, thus reducing the overall flux. In addition, the model is shown to exhibit sharp fronts moving with constant speed, another distinctive feature of non-Fickian polymer-penetrant systems.

1. Introduction

Over the last several decades, much work, both experimental and theoretical, has been devoted to the study of polymer-penetrant systems. One

Address for correspondence: Professor D. A. Edwards, Department of Mathematics, University of Maryland, College Park, College Park, MD 20742-4015. E-mail: dae@math.umd.edu.

STUDIES IN APPLIED MATHEMATICS 99:49–80

Published by Blackwell Publishers, 350 Main Street, Malden, MA 02148, USA, and 108 Cowley Road, Oxford, OX4 1JF, UK.

anomalous feature of such systems is a change of state in the polymer from a *rubbery* state (denoted by sub- and superscripts r) when the polymer is nearly saturated, to a *glassy* state (denoted by sub- and superscripts g) when the polymer is nearly dry. When a saturated polymer film or fiber is desorbed, often a glassy region develops at the exposed surface. Since the polymer is now in two states—the glassy skin and the deeper rubbery material—this phenomenon is called *literal skinning* [1–3]. Because the diffusion coefficient in the glassy region is much lower than in the rubbery region, this skin will slow the desorption process [4].

This skinning process can be desirable for such processes as membrane production by phase inversion [5] or spray-drying operations [6]. In addition, the glassy skin can aid in the production of more effective protective clothing, equipment, or sealants [7–9]. However, polymer skinning is undesirable in coating processes due to nonuniformities in the polymer coating and a decrease in the drying rates [3].

An even more unusual phenomenon, called *trapping skinning*, can also occur. In trapping skinning, an increase in the force driving the desorption will actually *decrease* the accumulated flux through the boundary! This behavior cannot be described solely by the lower diffusion coefficient in the glassy region; other effects must be included [2, 3, 10]. Although all the physical mechanisms for such behavior are not known, most scientists agree that one dominant factor is a viscoelastic stress in the polymer. This stress is related to the *relaxation time*, which measures the time it takes one portion of the polymer entaglement network to react to changes in another portion. In certain polymer-penetrant systems, this stress, which is a nonlinear memory effect, is as important to the transport process as the well-understood Fickian dynamics [11–13]. In the glassy region, the relaxation time is finite, so the stress is an important effect. In the rubbery region, the relaxation time is nearly instantaneous; hence, the memory effect is not as important there [8, 11, 14].

In this article, we undertake a study of a previously derived model [15, 16] to explain this anomalous Case II behavior. The model consists of a set of coupled partial-differential equations. The moving boundary-value problem that results cannot be solved by similarity solutions, but can be solved using asymptotic and singular perturbation techniques.

Since we are modeling desorption of a substance from a polymer film, two important measurable quantities can be identified: the speed of the front separating the glassy and rubbery regions and the flux of the penetrant through the exposed boundary. In our analysis, each of these quantities is identified and related to the dimensionless parameters. These computations should provide useful information to chemical engineers who wish to verify our model experimentally and, if our model is shown to be accurate, to those who wish to exploit the skinning phenomenon for their own purposes.

2. Governing equations

We begin with our theoretical equations for diffusion:

$$\tilde{C}_{\tilde{t}} = \left[\tilde{D}(\tilde{C})\tilde{C}_{\tilde{x}} + E\tilde{\sigma}_{\tilde{x}}\right]_{\tilde{x}}, \tag{2.1a}$$

$$\tilde{\sigma}_{\tilde{t}} + \beta(\tilde{C})\,\tilde{\sigma} = \mu\tilde{C} + \nu\tilde{C}_{\tilde{t}}, \tag{2.1b}$$

where $\tilde{C}$ is the concentration of the penetrant, $\tilde{D}(\tilde{C})$ is the molecular diffusion coefficient, $\beta(\tilde{C})$ is the inverse of the relaxation time, and μ, ν, and E are positive constants. Although these equations are derived in detail in [15], a brief summary is appropriate. Equation (2.1a) comes from assuming the chemical potential depends not only on $\tilde{C}$, but also on the nonstate variable $\tilde{\sigma}$, which includes memory effects into our diffusive flux. Since the evolution equation (2.1b) for $\tilde{\sigma}$ is reminiscent of the one for viscoelastic stress, we refer to $\tilde{\sigma}$ as a "stress" throughout this work. Equations (2.1) have been successfully used in [15, 17–19] to model various types of anomalous behavior in polymer-penetrant systems.

In many polymer-penetrant systems, $\beta(\tilde{C})$ changes greatly as the polymer goes from the glassy state to the rubbery state [8, 11, 14, 20, 21]. However, the differences in $\beta(\tilde{C})$ *within* phases are qualitatively negligible when compared with the differences *between* phases. Hence, we model $\beta(\tilde{C})$ by its average in each phase, yielding the following functional form:

$$\beta(\tilde{C}) = \begin{cases} \beta_{\mathrm{g}}, & 0 \le \tilde{C} \le \tilde{C}_{*}\ (\text{glass}), \\ \beta_{\mathrm{r}}, & \tilde{C}_{*} < \tilde{C} \le \tilde{C}_{\mathrm{c}}\ (\text{rubber}), \end{cases} \tag{2.2}$$

where $\tilde{C}_{*}$ is the concentration at which the rubber–glass transistion occurs and $\tilde{C}_{\mathrm{c}}$ is the saturation level for the polymer.

We wish to model the desorption of an initially saturated semi-infinite polymer, so we have that

$$\tilde{C}(\tilde{x},0) = \tilde{C}_{\mathrm{c}}. \tag{2.3a}$$

We also need an initial condition for the stress, but we do not wish to impose it at this time, so we simply let

$$\tilde{\sigma}(\tilde{x},0) = \tilde{\sigma}_{i}(\tilde{x},0). \tag{2.3b}$$

At the exposed edge ($\tilde{x} = 0$), we apply a *radiation condition*, which indicates that the flux through the inside of the film is proportional to the difference between the concentration at the edge of the film and the exterior concentration:

$$\tilde{J}(0,\tilde{t}) = -\left[\tilde{D}(\tilde{C})\tilde{C}_{\tilde{x}} + E\tilde{\sigma}_{\tilde{x}}\right](0,\tilde{t}) = \tilde{k}\left[\tilde{C}_{\text{ext}} - \tilde{C}(0,\tilde{t})\right],$$

where $\tilde{k} > 0$ is a measure of the permeability of the outer surface. We assume that $\tilde{C}_{\text{ext}} = 0$, so we have

$$\left[\tilde{D}(\tilde{C})\tilde{C}_{\tilde{x}} + E\tilde{\sigma}_{\tilde{x}}\right](0,\tilde{t}) = \tilde{k}\tilde{C}(0,\tilde{t}). \tag{2.4}$$

Note that (2.4) implies that the flux desorbed depends directly on the concentration at the boundary. Therefore, we see that if the boundary is dry (i.e., if a skin has formed), then there will be very little flux through the boundary and the penetrant will be trapped inside the polymer.

To understand these dynamics better, it is instructive to define the *accumulated concentration flux* $\tilde{F}$:

$$\tilde{F} \equiv \int_0^{\infty} \tilde{D}(\tilde{C})\tilde{C}_{\tilde{x}}(0,\tilde{t})\, d\tilde{t}. \tag{2.5}$$

Not only is $\tilde{F}$ an easy quantity to measure experimentally, but also its behavior will determine whether we have trapping skinning, where an increase in the driving force (in this case, represented by $\tilde{k}$) will actually produce a *decrease* in $\tilde{F}$.

Our problem will involve matching the solutions of the two equations where $\beta = \beta_{\text{g}}$ and $\beta = \beta_{\text{r}}$. Thus, it is necessary to impose conditions at the moving boundary $\tilde{s}(\tilde{t})$ between the two regions. We begin by assuming continuity of concentration at the specified transition value $\tilde{C}_*$:

$$\tilde{C}^{\text{r}}(\tilde{s}(\tilde{t}),\tilde{t}) = \tilde{C}_* = \tilde{C}^{\text{g}}(\tilde{s}(\tilde{t}),\tilde{t}). \tag{2.6}$$

In addition, we assume that the stress is continuous there, although we need not impose a specific value:

$$\tilde{\sigma}^{\text{r}}(\tilde{s}(\tilde{t}),\tilde{t}) = \tilde{\sigma}^{\text{g}}(\tilde{s}(\tilde{t}),\tilde{t}). \tag{2.7}$$

Lastly, we need to account for the fundamental change, seen experimentally, that takes place in the polymer as it changes from glass to rubber. Experimentally, this has been shown to be related to a stretching of the

polymer. The penetrant used up by the polymer in this stretching is directly analogous to the energy used up in melting in a standard two-phase heat conduction problem. Hence, we follow the same sort of derivation. Given the general form that $\tilde{C}_{\tilde{t}} = -\tilde{J}_{\tilde{x}}$, where $\tilde{J}$ is the flux, we use the standard condition that the difference between the flux in and the flux out is proportional to the speed of the front, i.e.,

$$\left[\tilde{J}\right]_{\tilde{s}} = -\tilde{a}\frac{d\tilde{s}}{d\tilde{t}},$$

where $\tilde{a}$ is a material constant and where we have defined the operator $[f]_{\tilde{s}} \equiv f^{g}(\tilde{s}^{-}(\tilde{t}),\tilde{t}) - f^{r}(\tilde{s}^{+}(\tilde{t}),\tilde{t})$. Note that $\tilde{a}$ plays the same role as the latent heat in a Stefan problem. However, it is shown later that such a simple interpretation of $\tilde{a}$ is inappropriate. Substituting our expression for $\tilde{J}$ from (2.1a), we have the following:

$$\left[\tilde{D}(\tilde{C})\tilde{C}_{\tilde{x}} + E\tilde{\sigma}_{\tilde{x}}\right]_{\tilde{s}} = \tilde{a}\frac{d\tilde{s}}{d\tilde{t}}. \tag{2.8}$$

When introducing nondimensional variables into the problem, we wish to let our independent variables vary on a physically observable time scale. Since the relaxation time in the glassy polymer is on the order of seconds and hence physically realizable, we use β_g to normalize our time scale. We also choose a length scale given by the glassy polymer to normalize our length scale. In summary, we have

$$x = \tilde{x}\sqrt{\frac{\beta_g}{\nu E}}, \qquad t = \tilde{t}\beta_g, \qquad s(t) = \frac{\tilde{s}(\tilde{t})}{\tilde{x}_c}, \qquad C(x,t) = \frac{\tilde{C}(\tilde{x},\tilde{t})}{\tilde{C}_c},$$

$$\sigma(x,t) = \frac{\tilde{\sigma}(\tilde{x},\tilde{t})}{\nu\tilde{C}_c}, \qquad \sigma_i(x) = \frac{\tilde{\sigma}_i(\tilde{x})}{\nu\tilde{C}_c}, \qquad C_* = \frac{\tilde{C}_*}{\tilde{C}_c}, \qquad a = \frac{\tilde{a}}{\tilde{C}_c},$$

$$k = \frac{\tilde{k}}{\sqrt{\nu E\beta_g}}, \qquad D(C) = \frac{\tilde{D}(\tilde{C})}{\nu E}, \qquad F = \frac{\tilde{F}}{\tilde{C}_c}\sqrt{\frac{\beta_g}{\nu E}}.$$

Then Equations (2.1)–(2.4) and (2.6)–(2.8) reduce to

$$C_t = \left[D(C)C_x + \sigma_x\right]_x, \tag{2.9a}$$

$$\sigma_t + \frac{\beta}{\beta_g}\sigma = \frac{\mu}{\nu\beta_g}C + C_t, \tag{2.9b}$$

$$C(x,0) = 1, \tag{2.10a}$$

$$\sigma(x,0) = \sigma_i(x), \tag{2.10b}$$

$$D(C)C_x(0,t) + \sigma_x(0,t) = kC(0,t), \tag{2.11}$$

$$C^{\mathrm{r}}(s(t),t) = C_* = C^{\mathrm{g}}(s(t),t), \tag{2.12}$$

$$\sigma^{\mathrm{r}}(s(t),t) = \sigma^{\mathrm{g}}(s(t),t), \tag{2.13}$$

$$\left[D(C)C_x + \sigma_x\right]_s = a\dot{s}, \tag{2.14}$$

where the dot indicates differentiation with respect to t. These are the equations that we will be using in our nonlinear analysis. Once we have computed our solutions, we will use them to calculate our nondimensional accumulated concentration flux:

$$F = \int_0^\infty D(C)C_x(0,t)\,dt. \tag{2.15}$$

To make the problem analytically tractable, we make one more simplifying assumption. The molecular diffusion coefficient $D(C)$ often increases dramatically as the polymer goes from the glassy to rubbery state [21]. However, changes *within* phases are less important. Hence, we perform the same averaging as we did with the relaxation time to obtain the following form for $D(C)$:

$$D(C) = \begin{cases} D_{\mathrm{g}}, & 0 \le C \le C_*, \\ D_{\mathrm{r}}, & C_* \le C \le 1. \end{cases} \tag{2.16}$$

This piecewise-constant form for $D(C)$ has been used by Crank [22] to study these anomalous systems. More discussion of various physically appropriate forms for $D(C)$ can be found in Cohen and White [23].

Due to the forms of (2.2) and (2.16), we see that we may treat $\beta(C)$ and $D(C)$ as constants. Then (2.9a) becomes

$$C_t = D(C)C_{xx} + \sigma_{xx}. \tag{2.17}$$

Combining (2.17) and (2.9b) yields

$$C_{tt} = \left[1 + D(C)\right]C_{xxt} - \frac{\beta(C)}{\beta_{\mathrm{g}}}C_t + \left[\frac{\beta(C)D(C)}{\beta_{\mathrm{g}}} + \frac{\mu}{\nu\beta_{\mathrm{g}}}\right]C_{xx}. \tag{2.18}$$

It can be shown that (2.18) also holds for σ.

It has previously been shown [16] that our front condition (2.14) is equivalent to

$$\left[(D(C)+1)C_x\right]_s + \left(1-\frac{\beta_r}{\beta_g}\right)\frac{\sigma(s(t),t)}{\dot{s}} = a\dot{s}. \tag{2.19}$$

The second term on the left-hand side of (2.19) is highly unusual and results from solving (2.9b) for σ and using the results in (2.14). Due to the presence of this term, a standard similarity-solution approach is fruitless.

Finally we examine the relative size of our parameters. Experimentally it has been shown that polymers have a near-instantaneous relaxation time in the rubbery state, while in the glassy state these substances are characterized by finite relaxation times. Hence, we assume that $\beta_g / \beta_r = \epsilon$, where $0 < \epsilon \ll 1$. This is consistent with the observation that a polymer that has a near-instantaneous relaxation time will develop only a very thin skin [5].

In addition, we know that the diffusion coefficient also varies greatly between phases. It is known that in the glassy polymer skin the diffusion coefficient is small [4]. Therefore, we set $D_g = D_0\epsilon$. The small size of D_g shows that in the glassy region, the dominant contribution to the normalized flux is given by the stress term. This agrees with our understanding that the nonlinear relaxation effects arising from the stress are most pronounced in the glassy region. We expect the effects of the concentration to be dominant when determining the stress, so we let $\mu = \mu_0\epsilon^{-1}$. Finally, for reasons that become clear later, we require that

$$a < -1. \tag{2.20}$$

This requirement indicates that a cannot be interpreted in terms of the latent heat, since in this case the phase change parameter is negative. However, a restriction of the form of (2.20) is not uncommon for the model equations (2.1); a has been negative in other considerations of these equations [15].

Making these substitutions into (2.18) and (2.9b), we have the following in the glassy region:

$$C_{tt}^g = (1+D_0\epsilon)C_{xxt}^g - C_t^g + \left(D_0\epsilon + \frac{\gamma}{\epsilon}\right)C_{xx}^g, \tag{2.21a}$$

$$\sigma_t^g + \sigma^g = \frac{\gamma}{\epsilon}C^g + C_t^g, \tag{2.21b}$$

where

$$\gamma = \frac{\mu_0}{\nu\beta_g}.$$

Since (2.18) also holds for σ, we see from (2.21a) that we have the following equation for the stress in the glassy region:

$$\sigma_{tt}^g = (1 + D_0\epsilon)\sigma_{xxt}^g - \sigma_t^g + \left(D_0\epsilon + \frac{\gamma}{\epsilon}\right)\sigma_{xx}^g. \tag{2.22}$$

In addition, we have the following in the rubbery region:

$$C_{tt}^r = \alpha C_{xxt}^r - \frac{1}{\epsilon}C_t^r + \frac{\kappa^2}{\epsilon}C_{xx}^r, \tag{2.23a}$$

$$\sigma_t^r + \frac{1}{\epsilon}\sigma^r = \frac{\gamma}{\epsilon}C^r + C_t^r, \tag{2.23b}$$

where

$$\alpha = 1 + D_r, \qquad \kappa^2 = D_r + \gamma. \tag{2.23c}$$

In addition, Equation (2.19) becomes

$$(D_0\epsilon + 1)C_x^g(s(t),t) - \alpha C_x^r(s(t),t) + \left(1 - \frac{1}{\epsilon}\right)\frac{\sigma(s(t),t)}{\dot{s}} = a\dot{s}. \tag{2.24}$$

If the outer boundary is in the rubbery region, Equation (2.11) becomes

$$D_r C_x^r(0,t) + \sigma_x^r(0,t) = kC^r(0,t), \tag{2.25a}$$

while if it is in the glassy region we have

$$D_0\epsilon C_x^g(0,t) + \sigma_x^g(0,t) = kC^g(0,t). \tag{2.25b}$$

3. Outer solutions and the accumulated flux

We begin by constructing the solution in the rubbery region. We postulate the following expansions in ϵ for our functions:

$$C^r \sim C^{0r} + \epsilon C^{1r} + o(\epsilon), \qquad \sigma^r \sim \sigma^{0r} + \epsilon\sigma^{1r} + o(\epsilon). \tag{3.1}$$

Then in the rubbery region, Equations (2.23a) and (2.23b) become, to leading orders,

$$C_t^{0r} = \kappa^2 C_{xx}^{0r}, \tag{3.2a}$$

$$\sigma_t^{0r} + \frac{1}{\epsilon}(\sigma^{0r} + \epsilon\sigma^{1r}) = \frac{\gamma}{\epsilon}(C^{0r} + \epsilon C^{1r}) + C_t^{0r}. \tag{3.2b}$$

At the beginning of the problem, we expect the entire polymer to be rubbery. Therefore, we begin by solving (3.2) subject to (2.25a). Matching the ϵ^{-1} terms in (3.2b), we have

$$\sigma^{0r} = \gamma C^{0r}. \tag{3.3}$$

Hence for consistency we should set

$$\sigma_i(x) = \gamma. \tag{3.4}$$

If we do not define $\sigma_i(x)$ as in (3.4), we will have a thin initial layer of width ϵ where the stress would equilibrate to γ. Since this region is not of physical interest, we use (3.4) for our initial condition and do not consider the initial layer.

Substituting (3.3) into (2.25a), we have the following:

$$\kappa^2 C_x^{0r}(0,t) = kC^{0r}(0,t). \tag{3.5}$$

To complete our problem, we simply rewrite the leading order of (2.10a):

$$C^{0r}(x,0) = 1. \tag{3.6}$$

The solution of (3.2a), (3.5), and (3.6) is given by

$$C^{0r}(x,t) = C^k(x,t), \tag{3.7a}$$

where

$$C^k(x,t) = \operatorname{erf}\left(\frac{x}{2\kappa\sqrt{t}}\right) + \exp\left(\frac{kx + k^2 t}{\kappa^2}\right)\operatorname{erfc}\left(\frac{2kt + x}{2\kappa\sqrt{t}}\right). \tag{3.7b}$$

On the boundary we have

$$C^{0\mathrm{r}}(0,t) = \exp\left(\frac{k^2 t}{\kappa^2}\right)\operatorname{erfc}\left(\frac{k\sqrt{t}}{\kappa}\right), \tag{3.8}$$

which is a monotonically decreasing function of t, as we would expect. Therefore, we note that at some time t_*, given by

$$\exp\left(\frac{k^2 t_*}{\kappa^2}\right)\operatorname{erfc}\left(\frac{k\sqrt{t_*}}{\kappa}\right) = C_*,$$

the polymer will change from an all-rubbery to a two-phase state. Letting

$$z_* = \frac{k^2 t_*}{\kappa^2} \tag{3.9a}$$

to simplify our analysis, we have the implicit relation for z_*:

$$e^{z_*}\operatorname{erfc}\sqrt{z_*} = C_*. \tag{3.9b}$$

Note that z_* is a function of C_* only, as illustrated in Figure 1.

We now wish to make some initial asymptotic estimates for the time t_* for various C_*. If C_* is near 1 (that is, if the saturation concentration is very near the transition concentration) or $k/\kappa \ll 1$, a small-z_* asymptote is needed for the left-hand side of (3.9b), which yields

$$z_* \sim \frac{(1-C_*)^2\pi}{4}. \tag{3.10}$$

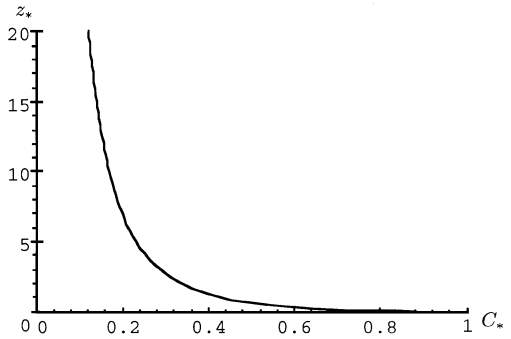

Figure 1. z_* vs C_*.

If C_* is near 0 or $k/\kappa \gg 1$, a large-z_* asymptote is needed for the left-hand side of (3.9b), and we have the following:

$$z_* \sim \frac{1}{C_*^2 \pi}. \tag{3.11}$$

To complete our work in this section, we use (3.7) in (3.3) to obtain σ^{0r}:

$$\sigma^{0r}(x,t) = \gamma\left[\operatorname{erf}\left(\frac{x}{2\kappa\sqrt{t}}\right) + \exp\left(\frac{kx + k^2 t}{\kappa^2}\right)\operatorname{erfc}\left(\frac{2kt + x}{2\kappa\sqrt{t}}\right)\right]. \tag{3.12}$$

Figure 2 shows a graph of $C^{0r}(x)$ vs x for the listed parameters and times. The concentration decreases monotonically with t, so the line $C^{0r} = 1$ corresponds to $t = 0$, and the graph where $C^{0r}(0,t) = 0.5 = C_*$ corresponds to t_*, the value of which was calculated numerically from (3.9). Since the polymer is totally in the rubbery state for $t < t_*$, the relaxation time is instantaneous, and there are no memory effects to consider. Thus, our solution behaves in a standard Fickian way and the concentration flux is $O(1)$. Note from (3.12) that for the particular value of γ we have chosen, Figure 2 is also a graph of $\sigma^{0r}(x)$.

At this time we consider the solution profile in the rubbery region when $t > t_*$. Now there are two phases in the polymer, and we are left to consider a moving boundary-value problem. To obtain a solution, we first see if there can be an interior layer near the moving front in C^{0r}. This would affect the boundary conditions for our outer solution. However, it can be shown that the equation in such a layer does not have a solution that remains bounded as $\zeta \to \infty$, which must occur for our solution to match.

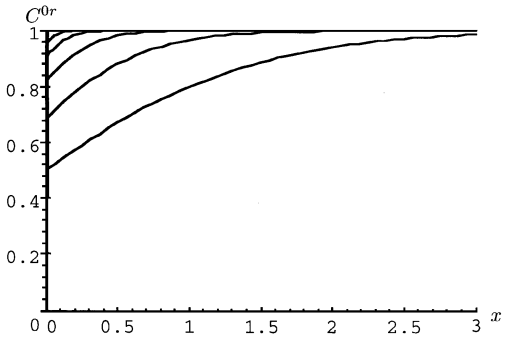

Figure 2. $C^{0r}(x)$ and $\sigma^{0r}(x)$ vs x for $\kappa = 2$, $k = 3$, $\gamma = 1$, $C_* = 0.5$, $t_* \approx 0.262$, and $t = 0$, 0.01, 0.04, 0.16, 0.64, and t_*.

Therefore, we see that there is no layer in this region, and our boundary condition (2.12) for $C^{\mathrm{r}}(s(t),t)$ must be satisfied exactly. Indeed, since we know that the same operator holds for C^{r} and σ^{r}, we know that we have no layer in σ^{r} either. Therefore, from (3.3) we have that

$$\sigma^{0\mathrm{r}}(s(t),t) = \gamma C_*, \tag{3.13}$$

and (2.24) becomes

$$(D_0\epsilon + 1)C_x^{\mathrm{g}}(s(t),t) - \alpha C_x^{\mathrm{r}}(s(t),t) + \left(1 - \frac{1}{\epsilon}\right)\frac{\gamma C_* + \epsilon\sigma^{1\mathrm{r}}(s(t),t)}{\dot{s}} = a\dot{s}. \tag{3.14}$$

Next we define the variable $u = t - t_*$. To solve for our solution, we employ the integral method developed by Boley [24] for simpler diffusion problems and used extensively by Edwards and Cohen on Equations (2.1) [15, 17, 19]. In this method, we assume that the equations for the rubbery region hold for the *entire* semi-infinite region for some function $T(x,u)$. Next we impose a *fictitious* boundary condition involving an unknown function $f(u)$ at $x = 0$ for $u > 0$. We then require this solution to satisfy all the other true boundary conditions. This solution will then give the proper result in its region of validity, $x > s(t)$. Since we know that $C^k(x,t)$ is a solution to (3.2a) that solves our initial condition and the fictitious condition $f(u) = 0$, we let

$$C^{0\mathrm{r}}(x,t) = T(x,u + t_*) + C^k(x,t), \qquad x > s(t), \tag{3.15a}$$

in which case Equations (3.2a), (3.5), and (3.6) become

$$T_u = \kappa^2 T_{xx}, \qquad x > 0, u > 0, \tag{3.15b}$$

$$\kappa^2 T_x(0,u) = kT(0,u) + f(u), \tag{3.16}$$

$$T(x,0) = 0. \tag{3.17}$$

The solution of Equations (3.15b)–(3.17) is given by

$$T(x,u) = -\frac{1}{\kappa}\int_0^u f(u-\tau) \times\left[\frac{1}{\sqrt{\pi\tau}}\exp\left(-\frac{x^2}{4\kappa^2\tau}\right) - \frac{k}{\kappa}\exp\left(\frac{kx + k^2\tau}{\kappa^2}\right)\operatorname{erfc}\left(\frac{2k\tau + x}{2\kappa\sqrt{\tau}}\right)\right] d\tau. \tag{3.18}$$

Inserting (3.18) into (3.15a), we have

$$C^{0r}(x,t) = -\frac{1}{\kappa}\int_0^u f(u-\tau) \times\left[\frac{1}{\sqrt{\pi\tau}}\exp\left(-\frac{x^2}{4\kappa^2\tau}\right)-\frac{k}{\kappa}\exp\left(\frac{kx+k^2\tau}{\kappa^2}\right)\operatorname{erfc}\left(\frac{2k\tau+x}{2\kappa\sqrt{\tau}}\right)\right]d\tau + C^k(x,t), \qquad x > s(t). \tag{3.19}$$

Using this expression in (2.12) gives us the first condition on s and f:

$$C_* = -\frac{1}{\kappa}\int_0^u f(u-\tau) \times\left[\frac{1}{\sqrt{\pi\tau}}\exp\left(-\frac{s^2}{4\kappa^2\tau}\right)-\frac{k}{\kappa}\exp\left(\frac{ks+k^2\tau}{\kappa^2}\right)\operatorname{erfc}\left(\frac{2k\tau+s}{2\kappa\sqrt{\tau}}\right)\right]d\tau + C^k(s,t). \tag{3.20}$$

To satisfy Equation (3.14), we also need the value of $C_x^{0r}(s(t),t)$, so we calculate the derivative of each of its component parts:

$$C_x^k(s(t),t) = \frac{k}{\kappa^2}\exp\left(\frac{ks+k^2t}{\kappa^2}\right)\operatorname{erfc}\left(\frac{2kt+s}{2\kappa\sqrt{t}}\right), \tag{3.21a}$$

$$T_x(s(t),t) = -\frac{1}{\kappa^3}\int_0^u f(u-\tau)\left\{\frac{1}{\sqrt{\pi\tau}}\exp\left(-\frac{s^2}{4\kappa^2\tau}\right)\left(k-\frac{s}{2\tau}\right) - \frac{k^2}{\kappa}\exp\left(\frac{ks+k^2\tau}{\kappa^2}\right)\operatorname{erfc}\left(\frac{2k\tau+s}{2\kappa\sqrt{\tau}}\right)\right\}d\tau. \tag{3.21b}$$

Next we examine the glassy region. Letting

$$C^g(x,t) \sim C^{0g}(x,t) + \epsilon C^{1g}(x,t) + o(\epsilon),$$
$$\sigma^g(x,t) \sim \epsilon^{-1}\sigma^{0g}(x,t) + \sigma^{1g}(x,t) + o(1),$$

in (2.21), (2.22), (2.25b), and (3.14) yields

$$C_{tt}^{0g} = C_{xxt}^{0g} - C_t^{0g} + \frac{\gamma}{\epsilon}\left(C_{xx}^{0g} + \epsilon C_{xx}^{1g}\right), \tag{3.22a}$$

$$\epsilon^{-1}\sigma_t^{0g} + \sigma_t^{1g} + \epsilon^{-1}\sigma^{0g} + \sigma^{1g} = \frac{\gamma}{\epsilon}\left(C^{0g} + \epsilon C^{1g}\right) + C_t^{0g}, \tag{3.22b}$$

$$\sigma_{tt}^{0g} = \sigma_{xxt}^{0g} - \sigma_t^{0g} + \frac{\gamma}{\epsilon}\left(\sigma_{xx}^{0g} + \epsilon\sigma_{xx}^{1g}\right), \tag{3.23}$$

$$\epsilon^{-1}\sigma_x^{0g}(0,t) + \sigma_x^{1g}(0,t) = kC^{0g}(0,t), \tag{3.24}$$

$$(1+D_0\epsilon)\left(C_x^{0g} + \epsilon C_x^{1g}\right)(s(t),t) - \alpha C_x^{0r}(s(t),t)$$

$$+ \frac{1}{\dot{s}}\left(1-\frac{1}{\epsilon}\right)(\gamma C_* + \epsilon\sigma^{1r})(s(t),t) = a\dot{s}_0. \tag{3.25}$$

We immediately see that if $\sigma^{0g}(s(t),t) \neq 0$, then an interior layer is necessary around $x = s(t)$, since σ^{0g} is an order of magnitude larger than σ^{0r}. But it can be shown that there can be no interior layer there, and hence we have that

$$\sigma^{0g}(s(t),t) = 0. \tag{3.26}$$

It can also be shown that there is no boundary layer in (2.22) for σ^{0g} at $x = 0$, and so we must use the proper order of (3.24) for our boundary condition.

Taking the leading order of (3.23) and (3.24), we have

$$\sigma_{xx}^{0g} = 0, \qquad \sigma_x^{0g}(0,t) = 0,$$

which implies that the stress is a function of time only, so we have

$$\sigma^{0g}(x,t) \equiv 0. \tag{3.27}$$

Matching the ϵ^{-1} terms in (3.22b) yields

$$\sigma_t^{0g} + \sigma^{0g} = \gamma C^{0g}. \tag{3.28}$$

Using (3.27) in (3.28), we have that

$$C^{0g}(x,t) \equiv 0. \tag{3.29}$$

Since (2.22) will not support a boundary layer near $x = 0$, neither will (2.21a). Therefore, by using (3.29) in (2.15), we see that only $O(1)$ contribution to F comes from the range $0 \leq t \leq t_*$. However, we must be careful when neglecting the contribution from $t > t_*$ since we are integrating over an infinite range. We neglect this contribution after noting that in practice the experiment would end after some long (but finite) time and that our perturbation solution holds only in the limit that $\epsilon \to 0$. Therefore, we

replace (2.15) by

$$F = \int_0^{t_*} \frac{D_r k}{\kappa^2} C^{0r}(0,t)\, dt, \tag{3.30}$$

where we have used (3.5) and (3.29). Using (3.8) and (3.9) in (3.30), we have

$$F = \frac{D_r}{k}\left[2\sqrt{\frac{z_*}{\pi}} - (1 - C_*)\right]. \tag{3.31}$$

Therefore, we have the rather amazing result that for fixed C_*, an increase in k, which is the driving force for the desorption, will actually *decrease* F. This represents the phenomenon of trapping skinning [2, 4]. This rather counterintuitive result follows from the fact that z_* is a function of C_* only. Therefore, when we increase the driving force, the instantaneous flux increases, but by (3.9a) we see that t_* decreases. Since the range of integration decreases faster than the integrand increases, the accumulated flux decreases with increasing k.

Finally we consider the behavior of F as C_* takes on extremal values. Using (3.10) and (3.11), we obtain

$$F \sim \begin{cases} 0, & C_* \to 1, \\ \dfrac{2D_r}{kC_*\pi}, & C_* \to 0. \end{cases} \tag{3.32}$$

Therefore, we see that if the transition concentration is very near the saturation concentration, there is little time for the penetrant in the rubbery region to diffuse through the exposed surface, and hence F is small. On the other hand, if the transition concentration is low, the polymer is in the rubbery region for a long period of time, and hence F becomes arbitrarily large, which it can do since we have an infinite reservoir of penetrant.

4. Interior layers

Since our outer glassy solution given by (3.29) does not satisfy our front condition (2.12), we see that there must be an interior layer near $x = s(t)$. Letting

$$\zeta = \frac{x - s(t)}{\epsilon}, \qquad C^g(x,t) \sim C^{0-}(\zeta,t) + \epsilon C^{1-}(\zeta,t) + o(\epsilon), \tag{4.1}$$

in (2.21a), we have, to leading orders,

$$\dot{s}^2\epsilon^{-2}C^{0-}_{\zeta\zeta} = (1+D_0\epsilon)\left[-\epsilon^{-3}\dot{s}\left(C^{0-}_{\zeta\zeta\zeta}+\epsilon C^{1-}_{\zeta\zeta\zeta}\right)+\epsilon^{-2}C^{0-}_{\zeta\zeta t}\right] + \gamma\epsilon^{-3}\left(C^{0-}_{\zeta\zeta}+\epsilon C^{1-}_{\zeta\zeta}\right). \tag{4.2}$$

Matching the ϵ^{-3} terms, we have

$$C^{0-}(\zeta,t) = C_* e^{\gamma\zeta/\dot{s}}, \tag{4.3a}$$

$$C^{0g}(x,t) = C_* \exp\left[\frac{\gamma(x-s(t))}{\epsilon\dot{s}}\right], \tag{4.3b}$$

where we have used (3.29) for a matching condition and (2.12) for a boundary condition at $\zeta = 0$.

Since we see that $C^{0g}_x(s(t),t) = O(\epsilon^{-1})$, matching the ϵ^{-1} terms in (3.25) yields

$$C^{0g}_x(s(t),t) - \frac{\gamma C_*}{\epsilon\dot{s}} = 0. \tag{4.4}$$

Using (4.3b), we see that (4.4) is immediately satisfied. Hence, we see that in this case we must go to next order to obtain the functional form of $s(t)$, which will then provide us the final bit of information needed to construct the solution profiles.

It can be shown that another boundary layer of order ϵ will be needed for C^{1g}, so (3.25) becomes

$$C^{1-}_\zeta(0,t) - \alpha C^{0r}_x(s(t),t) + (1+D_0)\frac{\gamma C_*}{\dot{s}} - \frac{\sigma^{1r}(s(t),t)}{\dot{s}} = a\dot{s}, \tag{4.5}$$

where we have used (4.3a).

We begin by solving for $\sigma^{1r}(s(t),t)$, which is the true value at $x = s(t)$ since there are no interior layers in the rubbery region. Matching the $O(1)$ terms in (3.2b) and using (3.3), we have

$$\sigma^{1r}(s(t),t) = (1-\gamma)C^{0r}_t(s(t),t). \tag{4.6}$$

Taking the total derivative of (2.12) with respect to t, we have

$$C^{0r}_t(s(t),t) = -\dot{s}C^{0r}_x(s(t),t). \tag{4.7}$$

Using (4.7) in (4.6), we have

$$\sigma^{1\mathrm{r}}(s(t),t) = -(1-\gamma)\dot{s}C_x^{0\mathrm{r}}(s(t),t). \tag{4.8}$$

Substituting Equation (4.8) in (4.5) yields

$$C_\zeta^{1-}(0,t) - \kappa^2 C_x^{0\mathrm{r}}(s(t),t) + (1+D_0)\frac{\gamma C_*}{\dot{s}} = a\dot{s}, \tag{4.9}$$

where we have used (2.23c).

Next we continue by finding C^{1-}. Using our results for $C^{0\mathrm{g}}$ from (3.29) and $\sigma^{0\mathrm{g}}$ from (3.27) and matching the next-order terms in (3.22)–(3.24), we have

$$C_{xx}^{1\mathrm{g}} = 0, \tag{4.10a}$$

$$\sigma_t^{1\mathrm{g}} + \sigma^{1\mathrm{g}} = \gamma C^{1\mathrm{g}}, \tag{4.10b}$$

$$\sigma_{xx}^{1\mathrm{g}} = 0, \tag{4.11}$$

$$\sigma_x^{1\sigma}(0,t) = 0. \tag{4.12}$$

In addition, we have front conditions given by (3.13) and (2.12):

$$\sigma^{1\mathrm{g}}(s(t),t) = \sigma^{0\mathrm{r}}(s(t),t) = \gamma C_*, \tag{4.13a}$$

$$C^{1\mathrm{g}}(s(t),t) = 0. \tag{4.13b}$$

It can be shown that just as there is no boundary layer in $\sigma^{0\mathrm{g}}$ near $x=0$, neither is there one in $\sigma^{1\mathrm{g}}$. Therefore, from (4.11) and (4.12) we see that $\sigma^{1\mathrm{g}}$ must be a function of time only, so to calculate it we simply use (4.13a):

$$\sigma^{1\mathrm{g}}(x,t) \equiv \gamma C_*. \tag{4.14}$$

Substituting (4.14) into (4.10b), we have

$$C^{1\mathrm{g}}(x,t) \equiv C_*. \tag{4.15}$$

We see from (4.13b) that there must be a boundary layer around $x = s(t)$. Using the ϵ^{-2} terms in (4.2), we have

$$\dot{s}^2 C_{\zeta\zeta}^{0-} = -D_0\dot{s}C_{\zeta\zeta\zeta}^{0-} - \dot{s}C_{\zeta\zeta\zeta}^{1-} + C_{\zeta\zeta t}^{0-} + \gamma C_{\zeta\zeta}^{1-}. \tag{4.16}$$

Using (4.3b) in (4.16), matching to our outer solution given by (4.15), and solving our front condition (4.13b), we obtain

$$C^{1-}(\zeta,t) = -C_* \zeta e^{\gamma\zeta/\dot{s}}\left(\frac{D_0\gamma}{\dot{s}} + \dot{s} + \frac{\gamma\ddot{s}\zeta}{2\dot{s}^3}\right) + C_*(1-e^{\gamma\zeta/\dot{s}}). \quad (4.17)$$

Summarizing our results, we have

$$C^{\mathrm{g}}(x,t) = C_* \exp\left[\frac{\gamma(x-s(t))}{\epsilon\dot{s}}\right] \times\left\{1-\epsilon-[x-s(t)]\left(\frac{D_0\gamma}{\dot{s}} + \dot{s} + \frac{\gamma\ddot{s}[x-s(t)]}{2\epsilon\dot{s}^3}\right)\right\} + \epsilon C_* + o(\epsilon), \quad (4.18)$$

$$\sigma^{\mathrm{g}}(x,t) = C_*\gamma + o(1). \quad (4.19)$$

Now that we have $C^{1-}(\zeta,t)$, we must calculate its derivative at $\zeta = 0$ to use in (4.9):

$$C^{1-}_{\zeta}(0,t) = -\frac{C_*\gamma}{\dot{s}}(1+D_0) - C_*\dot{s}. \quad (4.20)$$

Substituting (4.20) into (4.9) yields

$$C^{0\mathrm{r}}_x(s(t),t) = -\frac{a+C_*}{\kappa^2}\dot{s}. \quad (4.21)$$

Since we know that both $\dot{s}$ and $C^{0\mathrm{r}}_x(s(t),t)$ are positive, we see that the coefficient of $\dot{s}$ must be positive. Since $C_* < 1$, we see that (2.20) is sufficient for this to be true.

The last pieces needed to solve (4.21) are given by (3.21). Solving (4.21) simultaneously with (3.20) will complete our solution. In the next two sections, we provide small and large asymptotic results for f (and hence $C^{0\mathrm{r}}$) and $s(t)$.

5. Near the transition time

We now obtain asymptotic estimates of our functions near (but after) the transition time t_*. To do this, we make the following substitution:

$$s(t) = S(u) \sim s_0 u^m \qquad \text{as } u \to 0^+, \quad (5.1)$$

where $m > 0$ since $s(t_*) = S(0) = 0$. Using (5.1) in (3.21a), we obtain

$$C_x^k(S(u),u) \sim \frac{k}{\kappa^2}\exp\left[\frac{ks_0u^m + k^2(t_* + u)}{\kappa^2}\right]\operatorname{erfc}\left[\frac{2k(t_* + u) + s_0u^m}{2\kappa\sqrt{t_* + u}}\right]$$

$$\sim \frac{k}{\kappa^2}\left[C_* + \frac{ku}{\kappa}\left(\frac{C_*k}{\kappa} - \frac{1}{\sqrt{\pi t_*}}\right) + \frac{s_0u^m}{\kappa}\left(\frac{C_*k}{\kappa} + \frac{1}{\sqrt{\pi t_*}}\right)\right], \tag{5.2}$$

where we have used (3.9). Using (5.1) in (3.7b), we have that

$$C^k(S(u),u) \sim \operatorname{erf}\left(\frac{s_0u^m}{2\kappa\sqrt{t_* + u}}\right)$$

$$+ \left[C_* + \frac{ku}{\kappa}\left(\frac{C_*k}{\kappa} - \frac{1}{\sqrt{\pi t_*}}\right) + \frac{s^0u^m}{\kappa}\left(\frac{C_*k}{\kappa} - \frac{1}{\sqrt{\pi t_*}}\right)\right]$$

$$\sim C_* + \frac{ku}{\kappa}\left(\frac{C_*k}{\kappa} - \frac{1}{\sqrt{\pi t_*}}\right) + \frac{C_*ks_0u^m}{\kappa^2}. \tag{5.3}$$

We see from (5.3) that we must have $T(S(u),u) = o(1)$ as $u \to 0$. Using (5.1) in (4.21), we have

$$C_x^{0r}(S(u),u) = -\frac{a + C_*}{\kappa^2}ms_0u^{m-1}. \tag{5.4}$$

We assume that

$$f(u) \sim f_0u^n \qquad \text{as } u \to 0. \tag{5.5}$$

Our next task is to determine the proper value of n. Physically, we should expect that our fictitious boundary condition should be continuous at t_*, namely that $f(0) = 0$. Since (3.15b) is a diffusion problem, we might expect our solution to depend on $u^{1/2}$. Choosing $n = 1/2$, we see that (3.18) and (3.21b) become

$$T_x(x,u) \sim \frac{f_0\sqrt{\pi}}{2k\kappa}\left[\operatorname{erfc}\left(\frac{S}{2\kappa\sqrt{u}}\right) - \exp\left(\frac{kS - k^2u}{\kappa^2}\right)\operatorname{erfc}\left(\frac{2ku + S}{2\kappa\sqrt{u}}\right)\right], \tag{5.6a}$$

$$T_x(S(u),u) \sim \frac{f_0u^{1/2}}{\kappa^2}. \tag{5.6b}$$

Thus, using (5.2), the leading order of (5.4) is

$$\frac{kC_*}{\kappa^2} = -\frac{a+C_*}{\kappa^2} m s_0 u^{m-1},$$

from which we have that

$$m = 1, \qquad s_0 = -\frac{kC_*}{a+C_*}. \tag{5.7}$$

Note that our initial front speed depends linearly on k; that is, a larger permeability coefficient at the boundary will cause a faster-moving glass–rubber transition front. In addition, we see that initially our phase-transition front moves with constant speed and is very sharp. This type of behavior, when seen in sorption experiments, is associated with Case II diffusion [14, 25].

To calculate f_0, we need $T(S(u),u)$, which we obtain by substituting (5.5) into (3.18):

$$T(x,u) \sim -\frac{f_0\sqrt{\pi}}{2\kappa}\left[\frac{\kappa^2}{k^2}\exp\left(\frac{kx+k^2u}{\kappa^2}\right)\operatorname{erfc}\left(\frac{2ku+x}{2\kappa\sqrt{u}}\right)\right.$$
$$\left.-\left(\frac{\kappa^2}{k^2}+\frac{x}{k}\right)\operatorname{erfc}\left(\frac{x}{2\kappa\sqrt{u}}\right)+\frac{2\kappa}{k}\sqrt{\frac{u}{\pi}}\exp\left(-\frac{x^2}{4\kappa^2 u}\right)\right]. \tag{5.8}$$

Using (5.1) (along with our knowledge that $m=1$) in (5.8), we have

$$T(S(u),u) \sim -\frac{f_0\sqrt{\pi}}{2\kappa}\left\{\frac{\kappa^2}{k^2}\exp\left[\frac{ku(s_0+k)}{\kappa^2}\right]\operatorname{erfc}\left[\frac{(2k+s_0)u^{1/2}}{2\kappa}\right]\right.$$
$$\left.-\left(\frac{\kappa^2}{k^2}+\frac{s_0u}{k}\right)\operatorname{erfc}\left(\frac{s_0u^{1/2}}{2\kappa}\right)+\frac{2\kappa}{k}\sqrt{\frac{u}{\pi}}\exp\left(-\frac{s_0^2u}{4\kappa^2}\right)\right\}$$
$$\sim -\frac{f_0u\sqrt{\pi}}{2\kappa}. \tag{5.9}$$

Using the fact that $m=1$ in (5.3), we have, to leading orders,

$$C^k(S(u),u) \sim C_* + \frac{ku}{\kappa}\left[\frac{C_*(k+s_0)}{\kappa} - \frac{1}{\sqrt{\pi t_*}}\right]. \tag{5.10}$$

Using (5.9) and (5.10) in (3.20), we have

$$f_0 = \frac{2k}{\sqrt{\pi}}\left[\frac{C_*(k+s_0)}{\kappa} - \frac{1}{\sqrt{\pi t_*}}\right]. \tag{5.11}$$

Summarizing our results, we have

$$t \to t_*^+, \qquad x > s(t),$$

$$\exp\left(\frac{k^2 t_*}{\kappa^2}\right)\operatorname{erfc}\left(\frac{k\sqrt{t_*}}{\kappa}\right) = C_*, \tag{5.12}$$

$$s(t) \sim s_0(t - t_*), \qquad s_0 = -\frac{kC_*}{a + C_*}, \tag{5.13}$$

$$\begin{aligned} C^{\mathrm{r}}(x,t) \sim\ & \operatorname{erf}\left(\frac{x}{2\kappa\sqrt{t}}\right) + \exp\left(\frac{kx + k^2 t}{\kappa^2}\right)\operatorname{erfc}\left(\frac{2kt + x}{2\kappa\sqrt{t}}\right) \\ & - \frac{1}{\kappa}\left[\frac{C_*(k+s_0)}{\kappa} - \frac{1}{\sqrt{\pi t_*}}\right] \\ & \times\left\{\frac{\kappa^2}{k}\exp\left[\frac{kx + k^2(t - t_*)}{\kappa^2}\right]\operatorname{erfc}\left[\frac{2k(t-t_*) + x}{2\kappa\sqrt{t - t_*}}\right] - \left(\frac{\kappa^2}{k} + x\right)\right. \\ & \left.\times\operatorname{erfc}\left(\frac{x}{2\kappa\sqrt{t - t_*}}\right) + 2\kappa\sqrt{\frac{t - t_*}{\pi}}\exp\left[-\frac{x^2}{4\kappa^2(t - t_*)}\right]\right\}. \end{aligned} \tag{5.14}$$

Figure 3 shows a graph of $C(x)$ vs x for small u and various parameters that satisfy (2.20). Since we are using a finite ϵ, we see that on a relatively

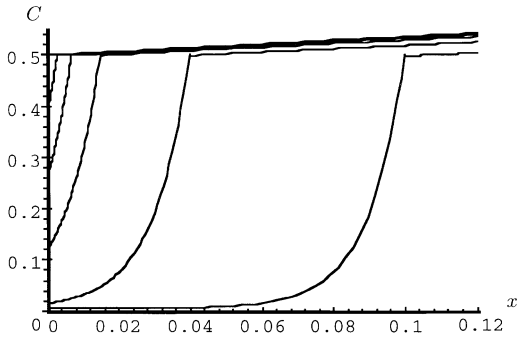

Figure 3. $C(x)$ vs x for $a = -2$, $D_0 = 2$, $\epsilon = 0.01$, $\kappa = 2$, $k = 3$, $\gamma = 1$, $C_* = 0.5$, $t_* \approx 0.262$, and $t - t_* \equiv u = 0$, 0.003, 0.007, 0.015, 0.04, and 0.1.

fast time scale (note that our largest $u = 0.1$) the concentration in the glassy region decays away to an $O(\epsilon)$ quantity. This is the mathematical manifestation of the formation of the glassy skin near the exposed surface. Note also that due to the small scale in the x-direction, our front is very sharp. This becomes more apparent in our long-time graphs.

Figure 4 shows $\sigma(x)$ vs x for the same parameters and times. We note that rather than decaying to zero, the stress in the glassy region remains at a constant value before making a smooth transition to the rubbery region. The gaps in the graph for the larger times is due to the fact that our asymptotic expansion for small times is starting to break down. Constructing further terms in the asymptotic expansions would yield new curves with less noticeable gaps.

6. Long-time asymptotics

We now obtain asymptotic estimates of our functions for large time. In the discussion that follows it is helpful to have the following asymptotic expansion, which holds for all x:

$$\exp\left(\frac{kx + k^2 t}{\kappa^2}\right)\operatorname{erfc}\left(\frac{2kt + x}{2\kappa\sqrt{t}}\right) \sim \frac{2\kappa\sqrt{t}}{(x + 2kt)\sqrt{\pi}}\exp\left(-\frac{x^2}{4\kappa^2 t}\right), \qquad t \to \infty. \tag{6.1}$$

We begin by making substitutions for large time,

$$s(t) = 2\kappa s_\infty t^j, \qquad f(t) \sim f_\infty t^p, \text{ as } t \to \infty, \tag{6.2}$$

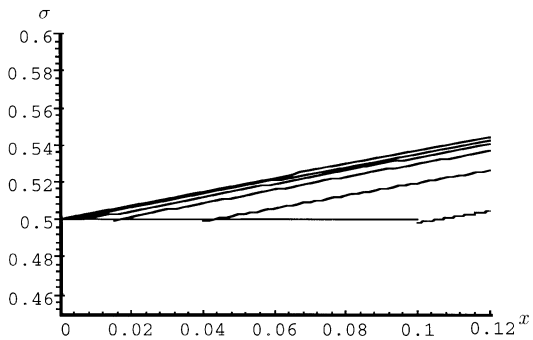

Figure 4. $\sigma(x)$ vs x for $a = -2$, $D_0 = 2$, $\epsilon = 0.01$, $\kappa = 2$, $k = 3$, $\gamma = 1$, $C_* = 0.5$, $t_* \approx 0.262$, and $t - t_* \equiv u = 0$, 0.003, 0.007, 0.015, 0.04, and 0.1.

where $j \geq 0$ since $\dot{s} > 0$. We would expect that $p \leq 0$ since this would force our solution to remain bounded. However, we do not postulate this; it follows from our analysis. Using our expression for $s(t)$ in (3.21a) and using (6.1), we obtain

$$C_x^k(s(t),t) \sim \frac{k \exp\left(-s_\infty^2 t^{2j-1}\right)}{\kappa\left(\kappa s_\infty t^{j-1/2} + k t^{1/2}\right)\sqrt{\pi}}. \tag{6.3}$$

Using our expression for $s(t)$ in (3.7b), we have

$$C^k(s(t),t) \sim \operatorname{erf}\left(s_\infty t^{j-1/2}\right) + \frac{\kappa \exp\left(-s_\infty^2 t^{2j-1}\right)}{\left(\kappa s_\infty t^{j-1/2} + k t^{1/2}\right)\sqrt{\pi}}. \tag{6.4}$$

First we assume that $j > \frac{1}{2}$. Then (6.4) becomes

$$C^k(s(t),t) \sim 1,$$

which means that we must have another $O(1)$ term to strike a balance in (3.20). However, note that $t \to \infty$ is the same as $u \to \infty$ in (3.18). Since this equation is diffusive in nature and hence has an underlying similarity variable $x/\sqrt{u}$, we see that for any n, the contribution from these terms would be *transcendentally* small for $j > \frac{1}{2}$. Therefore, we conclude that $j \not> \frac{1}{2}$.

Next we assume that $j < \frac{1}{2}$. Then for large t, $t^{j-1/2} \to 0$, so (6.4) becomes, to leading order,

$$C^k(s(t),t) \sim \frac{2 s_\infty}{t^{1/2-j}\sqrt{\pi}} + \frac{\kappa}{k\sqrt{\pi t}}, \tag{6.5}$$

which means once again that we must have another $O(1)$ term to strike a balance in (3.20). An $O(1)$ term can arise when $p = 0$, in which case Equation (3.18) becomes

$$T(x,u) \sim -\frac{f_\infty}{k}\left[\operatorname{erfc}\left(\frac{x}{2\kappa\sqrt{u}}\right) - \exp\left(\frac{kx + k^2 u}{\kappa^2}\right)\operatorname{erfc}\left(\frac{2ku + x}{2\kappa\sqrt{u}}\right)\right]. \tag{6.6}$$

Simplifications arise when we note from (3.7b) that

$$T(x,u) \sim -\frac{f_\infty\left[1 - C^k(x,u)\right]}{k}, \tag{6.7a}$$

$$T_x(x,u) \sim \frac{f_\infty C_x^k(x,u)}{k}. \tag{6.7b}$$

Therefore, (3.20) becomes, to leading order,

$$C_* \sim -\frac{f_\infty\left[1-C^k(s(t),t)\right]}{k} + C_k(s(t),t)$$

$$f_\infty = -kC_*. \tag{6.8}$$

Using (6.7b), (6.3), and (6.8) in (4.21), we have, to leading order,

$$C_x^k(s(t),t) + \frac{f_\infty C_x^k(s(t),t)}{k} = -\frac{a+C_*}{\kappa^2}\dot{s}$$

$$\frac{1-C_*}{\kappa\sqrt{\pi t}} = -\frac{2j(a+C_*)s_\infty t^{j-1}}{\kappa}. \tag{6.9}$$

Therefore, we see that to have a dominant balance, we must have $j=\frac{1}{2}$, which is not in agreement with our hypothesis that $j<\frac{1}{2}$. However, we retain our supposition that $p=0$.

Using these facts in (6.4) and (6.3), we have

$$C^k(s(t),t) \sim \operatorname{erf} s_\infty + \frac{\kappa\exp\left(-s_\infty^2\right)}{k\sqrt{\pi t}}, \tag{6.10a}$$

$$C_x^k(s(t),t) \sim \frac{\exp\left(-s_\infty^2\right)}{\kappa\sqrt{\pi t}}. \tag{6.10b}$$

Using (6.10) and (6.7) in (3.20) and (4.21), we have, to leading orders,

$$C_* \sim \operatorname{erf} s_\infty - \frac{f_\infty[1-\operatorname{erf} s_\infty]}{k}$$

$$f_\infty = \frac{k(\operatorname{erf} s_\infty - C_*)}{\operatorname{erfc} s_\infty}, \tag{6.11a}$$

$$\left(1+\frac{f_\infty}{k}\right)\frac{\exp\left(-s_\infty^2\right)}{\kappa\sqrt{\pi t}} = -\frac{(a+C_*)s_\infty}{\kappa\sqrt{t}}$$

$$\left(\frac{1-C_*}{\operatorname{erfc} s_\infty}\right)\frac{\exp\left(-s_\infty^2\right)}{s_\infty\sqrt{\pi}} = -(a+C_*)$$

$$g(s_\infty) \equiv \frac{1-C_*}{\sqrt{\pi}}\exp\left(-s_\infty^2\right) + (a+C_*)s_\infty \operatorname{erfc} s_\infty = 0. \tag{6.11b}$$

Now we search for roots of $g(s_\infty)$. We see that $g(0) > 0$ and note that

$$g(s_\infty) \sim \frac{1}{\sqrt{\pi}}\left(1 + a - \frac{a + C_*}{2s_\infty^2}\right)\exp\left(-s_\infty^2\right) \qquad \text{as } s_\infty \to \infty.$$

Therefore, we have the following:

$$g(s_\infty) \to \begin{cases} 0^+, & a \geq -1, \\ 0^-, & a < -1, \end{cases} \qquad \text{as } s_\infty \to \infty.$$

We next consider $g'(s_\infty)$, which is given by

$$g'(s_\infty) = -\frac{2s_\infty(1+a)}{\sqrt{\pi}}\exp\left(-s_\infty^2\right) + (a + C_*)\operatorname{erfc} s_\infty. \tag{6.12}$$

We see that if $a \geq -1$ then $g'(s_\infty) < 0$ for all s_∞, and (6.11b) has no root. Hence, we see that the condition for which a solution can exist is given by (2.20).

Is this solution unique? To answer this question, we note from the behavior of g at 0 and ∞ that there must be an odd number of roots. This odd number of roots means that $g'(s_\infty)$ must change sign at each root. Using (6.11b) in (6.12), we see that at a root $s_\infty = s_*$, we have

$$g'(s_*)\exp\left(s_*^2\right)s_*\sqrt{\pi} = 2s_*^2|1 + a| - (1 - C_*).$$

But we see that $g'(s_*)$ changes sign only once; hence, we have a unique root.

To obtain numerical results, we rewrite (6.11b) as

$$1 - C_*\left[1 - s_\infty(\operatorname{erfc} s_\infty)\exp\left(s_\infty^2\right)\sqrt{\pi}\right] \sim |a|s_\infty(\operatorname{erfc} s_\infty)\exp\left(s_\infty^2\right)\sqrt{\pi}. \tag{6.13}$$

We note that s_∞ does not depend on k. This is consistent with the observation that in a system of finite width, the steady-state skin depth does not depend appreciably on k [5].

Figure 5 shows a graph of the left- and right-hand sides of (6.13) for various allowable values of C_* and a. The value of s_∞ describing the front is given by the intersection of the two curves. We see that as C_* gets smaller, s_∞ gets smaller. This agrees with our intuition, as we expect that the front would slow as the rubber–glass transition value decreases. In addition, we see that as a increases, the front speed increases. This is because the absolute value of the jump in the flux needed to move the front along is decreasing, and hence the front should move faster.

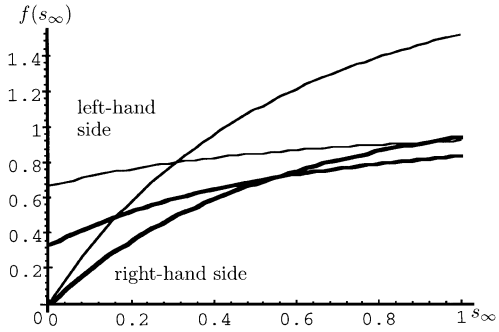

Figure 5. Left- and right-hand sides of (6.13). Light lines: $C_* = \frac{1}{3}$, $a = -2$. Dark lines: $C_* = \frac{2}{3}$, $a = -\frac{5}{4}$.

Summarizing our results, we have the following:

$$t \to \infty, \qquad x > s(t),$$

$$s(t) \sim 2\kappa s_\infty \sqrt{t}, \qquad \left(\frac{1 - C_*}{\operatorname{erfc} s_\infty}\right) \frac{\exp(-s_\infty^2)}{s_\infty \sqrt{\pi}} = -(a + C_*), \tag{6.14}$$

$$C^{0\mathrm{r}}(x,t) \sim \operatorname{erf}\left(\frac{x}{2\kappa\sqrt{t}}\right) + \exp\left(\frac{kx + k^2 t}{\kappa^2}\right) \operatorname{erfc}\left(\frac{2kt + x}{2\kappa\sqrt{t}}\right) + \frac{C_* - \operatorname{erf} s_\infty}{\operatorname{erfc} s_\infty}$$

$$\times \left[\operatorname{erfc}\left(\frac{x}{2\kappa\sqrt{t}}\right) - \exp\left(\frac{kx + k^2 t}{\kappa^2}\right) \operatorname{erfc}\left(\frac{2kt + x}{2\kappa\sqrt{t}}\right)\right], \tag{6.15}$$

$$\sigma^{\mathrm{r}}(x,t) \sim \gamma C^{\mathrm{r}}(x,t). \tag{6.16}$$

Figure 6 shows a graph of the short- and long-time expansions of our front position $s(t)$ in the $x = t$ plane. In addition, there is a darker curve,

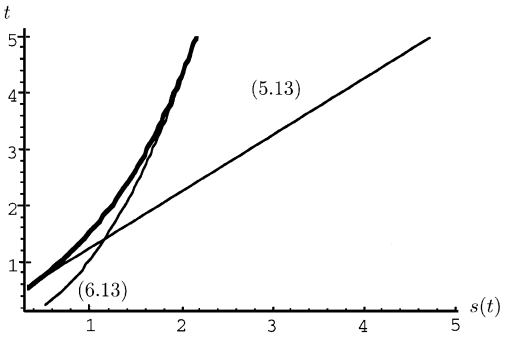

Figure 6. Short- and long-time asymptotes for $s(t)$ for $a = -2$, $D_0 = 2$, $\epsilon = 0.01$, $\kappa = 2$, $k = 3$, $\gamma = 1$, $C_* = 0.5$, and $t_* \approx 0.262$.

which interpolates between the two asymptotic expansions to show how the true front might behave. Note that the front slows as time increases.

Figure 7 shows a graph of $C(x)$ vs x for the same parameters as graphed earlier and for long times. Now it is much clearer that the front is sharp and quickly takes C^{g} from the transition value C_* to a value that is $O(\epsilon)$. The gaps for smaller times are once again indicative of the fact that our asymptotic expansion loses validity for smaller times. The mathematical interpretation of the skin is clear now, for we see the wide glassy region where there is practically no penetrant. We also see that the concentration flux through the exposed boundary is zero to the order of our approximation.

Figure 8 shows a graph of $\sigma(x)$ vs x for times and parameters the same as those in Figure 7. We once again note that the rubbery portion of the graph is the same as that for the concentration since $\gamma = 1$. We see that the stress in the glassy region remains at a constant value, which smoothly transitions in a Fickian way to the fully stressed polymer when $x \to \infty$. Thus we see that not only is the concentration flux zero at the boundary, but the total flux is zero there as well.

7. Conclusions

In the phenomenon of trapping skinning, several anomalous features of polymer-penetrant systems combine to yield a counterintuitive result: namely, that an increase in the driving force for desorption will actually decrease the amount of penetrant desorbed. As the penetrant is desorbed, a glassy skin forms at the exposed surface. Since the molecular diffusion coefficient is smaller in the glassy region [1–3], the formation of such a skin slows

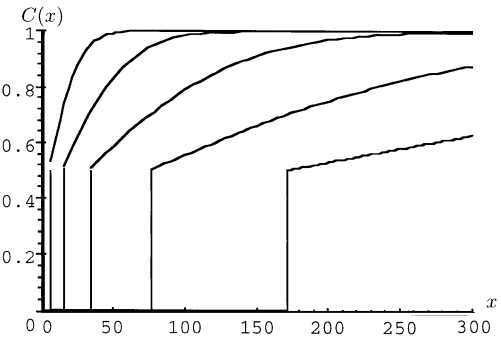

Figure 7. $C(x)$ vs x for $a = -2$, $D_0 = 2$, $\epsilon = 0.01$, $\kappa = 2$, $k = 3$, $\gamma = 1$, $C_* = 0.5$, $t = 50$, 250, 1250, 6250, and 31250.

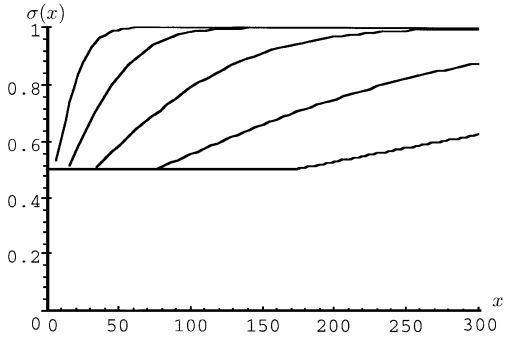

Figure 8. $\sigma(x)$ vs x for $a = -2$, $D_0 = 2$, $\epsilon = 0.01$, $\kappa = 2$, $k = 3$, $\gamma = 1$, $C_* = 0.5$, $t = 50$, 250, 1250, 6250, and 31250.

desorption [4]. However, the lower diffusion coefficient is not adequate to describe such behavior; rather, nonlinear viscoelastic effects must also be considered [2, 3, 10].

A mathematical model that captures this behavior was presented. The model, which contains memory effects, led to a set of coupled partial differential equations along with an unusual condition at the moving front $s(t)$ between the glassy and rubbery phases. The problem was not solvable by similarity solutions, and thus an integral method [24] had to be used to obtain asymptotic solutions.

Since the polymer is initially saturated and in the rubbery region, for a finite amount of time the polymer remained totally in the rubbery state. The concentration flux at the exposed surface was $O(1)$, and the solution behaved in a purely Fickian way. This is because memory effects are unimportant in the rubbery state [8].

Once the concentration at the boundary had reached C_*, the glass–rubber transition concentration, the character of the solution changed drastically. The glassy polymer could not support an $O(1)$ concentration, so an interior layer around $x = s(t)$ formed a sharp interface between the rubbery and glassy regions. This front initially moved with constant speed—behavior that, coupled with the sharp interface between the glassy and rubbery states, is reminiscent of Case II diffusion in sorption experiments [25].

A quantity of interest is the accumulated concentration flux F through the boundary, since this determines whether or not we are in the trapping skinning case. Since the concentration in the glassy polymer is $o(1)$, we see that the dominant contribution to F is from the rubbery region. As expected, the instantaneous flux through the boundary is increased when k, the driving force for the desorption, is increased. However, the duration of time during which the polymer is in the rubbery region (and hence the time

when there is an $O(1)$ contribution to F) decreases with increasing k. This duration effect is stronger, and hence we see that the overall accumulated flux decreases with k. This behavior embodies the very essence of trapping skinning.

8. Nomenclature

8.1. Variables and parameters

Units are listed in terms of length (L), mass (M), moles (N), or time (T). If the same letter appears both with and without tildes, the letter with a tilde has dimensions, while the letter without a tilde is nondimensionalized. The equation number where a particular quantity first appears is listed, if applicable.

$\tilde{a}$ coefficient in flux-front speed relationship, units N/L^3.
$\tilde{C}(\tilde{x},\tilde{t})$ concentration of penetrant at position $\tilde{x}$ and time $\tilde{t}$, units N/L^3 (2.1a).
$\tilde{D}(\tilde{C})$ binary diffusion coefficient for system, units L^2/T (2.1a).
E coefficient preceding the stress term in the modified diffusion equation, units NT/M (2.1a).
$\tilde{F}$ accumulated concentration flux through the boundary, units N/L^2 (2.5).
$f(u)$ fictitious boundary condition for T (3.16).
$g(s_\infty)$ function whose roots yield the coefficient of the long-time front position (6.11b).
$\tilde{J}(\tilde{x},\tilde{t})$ flux at position $\tilde{x}$ and time $\tilde{t}$, units N/L^2T.
j variable exponent for large-time asymptotics (6.2).
$\tilde{K}$ measure of permeability of outer surface, units L/T.
m variable exponent for small-time asymptotics (5.1).
n variable exponent for small-time asymptotics (5.5).
p variable exponent for large-time asymptotics (6.2).
$S(u)$ position of front in the u-coordinate system (5.1).
$\tilde{s}(\tilde{t})$ position of glass-rubber interface, defined as $\tilde{C}(\tilde{s}(\tilde{t}),\tilde{t}) = \tilde{C}_*$, units L (2.6).
T imbedding of C from one region to the fully semi-infinite region (3.15a).
$\tilde{t}$ time from imposition of external concentration, units T (2.1a).
u shifted time coordinate, defined by $u = t - t_*$ (3.15a).
$\tilde{x}$ distance from boundary, units L (2.1a).

Z the integers.
z scaled time variable, value $k^2 t/\kappa^2$ (3.9a).
α dimensionless parameter, defined as $\alpha = 1 + D_r$ (2.23a).
$\beta(\tilde{C})$ inverse of the relaxation time, units T^{-1} (2.1b).
γ nondimensional parameter, value $\mu_0/\nu\beta_g$ (2.21).
ϵ perturbation expansion parameter, value β_g/β_r.
ζ interior layer variable, defined as $[x - s(t)]/\epsilon$ (4.1).
κ nondimensional parameter, value $\sqrt{D_r + \gamma}$ (2.23c).
μ coefficient of concentration in stress evolution equation, units ML^2/NT^3 (2.1b).
ν coefficient of $\tilde{C}_{\tilde{t}}$ in stress evolution equation, units ML^2/NT^2 (2.1b).
$\tilde{\sigma}(\tilde{x}, \tilde{t})$ stress in polymer at position $\tilde{x}$ and time $\tilde{t}$, units M/LT^2 (2.1a).
τ dummy integration variable (3.18).

8.2. Other notation

c as a subscript, used to indicate the saturation concentration (2.2).
ext as a subscript, used to indicate a value exterior to the polymer.
g as a sub- or superscript, used to indicate the glassy state (2.2).
i as a subscript, used to indicate a quantity at $\tilde{t} = 0$ (2.3b).
$j \in Z$ as a sub- or superscript, used to indicate a term in an expansion, either in t or ϵ.
k as a superscript, used to indicate a known quantity (3.7a).
r as a sub- or superscript, used to indicate the rubbery state (2.2).
$\dot{\cdot}$ used to indicate differentiation with respect to t (2.14).
$*$ as a subscript, used to indicate a quantity at the transition value between the glassy and rubbery states (2.2).
$\bar{\cdot}$ as a superscript, used to indicate an interior layer near $x = s(t)$ in the glassy region (4.1).
∞ as a subscript, used to indicate a term in an expansion for large t (6.2).
$[\cdot]_{\tilde{s}}$ jump across the front $\tilde{s}$, defined as $\cdot^{g}(\tilde{s}^-(\tilde{t}), \tilde{t}) - \cdot^{r}(\tilde{s}^+(\tilde{t}), \tilde{t})$.

Acknowledgments

The author thanks Donald S. Cohen and Christopher Durning for their contributions, both direct and indirect, to this paper. This work was performed under National Science Foundation Grant DMS-9407531. Many of the calculations herein were performed using Maple.

References

1. R. A. Cairncross, L. F. Francis, and L. E. Scriven, Competing drying and reaction mechanisms in the formation of sol-to-gel films, fibers, and spheres, *Drying Tech. J.* 10:893–923 (1992).
2. R. A. Cairncross, L. F. Francis, and L. E. Scriven, Predicting drying in coatings that react and gel: Drying regime maps, *AIChE J.* 42:55–67 (1996).
3. R. A. Cairncross and C. J. Durning, A model for drying of viscoelastic polymer coatings, *AIChE J.*, 42:2415–2426 (1996).
4. G. W. Powers and J. R. Collier, Experimental modelling of solvent-casting thin polymer films, *Polymer Engrg. Sci.* 30:118–123 (1990).
5. J. E. Anderson and R. Ullman, Mathematical analysis of factors influencing the skin thickness of asymmetric reverse osmosis membranes, *J. Appl. Phys.* 44:4303–4311 (1973).
6. D. H. Charlesworth and W. R. Marshall, Jr., Evaporation from drops containing dissolved solids, *AIChE J.* 6:9–23 (1960).
7. C. A. Finch, Ed., *Chemistry and Technology of Water-Soluble Polymers*, Plenum, New York, 1983.
8. W. R. Vieth, *Diffusion in and through Polymers*: *Principles and Applications*, Oxford Univ. Press, Oxford, 1991.
9. J. S. Vrentas, C. M. Jorzelski, and J. L. Duda, A Deborah number for diffusion in polymer-solvent systems, *AIChE J.* 21:894–901 (1975).
10. J. Crank, The influence of concentration-dependent diffusion on rate of evaporation, *Proc. Phys. Soc.* 63:484–491 (1950).
11. H. L. Frisch, Sorption and transport in glassy polymers—A review, *Polymer Engrg. Sci.* 20:2–13 (1980).
12. D. R. Paul and W. J. Koros, Effect of partially immobilizing sorption on permeability and diffusion time lag, *J. Polym. Sci.* 14:675–685 (1976).
13. W. R. Vieth and K. J. Sladek, A model for diffusion in a glassy polymer, *J. Colloid Sci.* 20:1014–1033 (1965).
14. J. Crank, *The Mathematics of Diffusion*, 2nd ed., Oxford Univ. Press, Oxford, 1976.
15. D. A. Edwards and D. S. Cohen, A mathematical model for a dissolving polymer, *AIChE J.* 41:2345–2355 (1995).
16. D. A. Edwards and D. S. Cohen, An unusual moving boundary condition arising in anomalous diffusion problems, *SIAM J. Appl. Math.* 55:662–676 (1995).
17. D. A. Edwards, Constant front speed in weakly diffusive non-Fickian systems, *SIAM J. Appl. Math.* 55:1039–1058 (1995).
18. D. A. Edwards, Non-Fickian diffusion in thin polymer films, *J. Polym. Sci. B*: *Polym. Phys.* 34:981–997 (1996).
19. D. A. Edwards and D. S. Cohen, The effect of a changing diffusion coefficient in polymer-penetrant systems, *IMA J. Appl. Math.* 55:49–66 (1995).
20. C. Y. Hui, K. C. Wu, R. C. Lasky, and E. J. Kramer, Case II diffusion in polymers. I. Transient swelling, *J. Appl. Phys.* 61:5129–5136 (1987).
21. C. Y. Hui, K. C. Wu, R. C. Lasky, and E. J. Kramer, Case II diffusion in polymers. II. Steady state front motion, *J. Appl. Phys.* 61:5137–5149 (1987).
22. J. Crank, Diffusion in media with variable properties. III. Diffusion coefficients which vary discontinuously with concentration, *Trans. Faraday Soc.* 47:450–461 (1951).

23. D. S. COHEN and A. B. WHITE, JR., Sharp fronts due to diffusion and stress at the glass transition in polymers, *J. Polym. Sci. B: Polym. Phys.* 27:1731–1747 (1989).

24. B. A. BOLEY, A method of heat conduction analysis of melting and solidification problems, *J. Math. Phys.* 40:300–313 (1961).

25. N. THOMAS and A. H. WINDLE, Transport of methanol in poly-(methyl-methocrylate), *Polymer* 19:255–265 (1978).

UNIVERSITY OF MARYLAND AT COLLEGE PARK

(Received May 2, 1996)